

Room temperature magnetic stabilization of buried cobalt nanoclusters within a ferromagnetic matrix studied by soft x-ray magnetic circular dichroism

A. T. Hindmarch, K. J. Dempsey, J. P. Morgan, B. J. Hickey, D. A. Arena et al.

Citation: *Appl. Phys. Lett.* **93**, 172511 (2008); doi: 10.1063/1.3012368

View online: <http://dx.doi.org/10.1063/1.3012368>

View Table of Contents: <http://apl.aip.org/resource/1/APPLAB/v93/i17>

Published by the [American Institute of Physics](#).

Related Articles

Effect of molecule-particle binding on the reduction in the mixed-frequency alternating current magnetic susceptibility of magnetic bio-reagents

J. Appl. Phys. **112**, 024704 (2012)

Energy dissipation and switching delay in stress-induced switching of multiferroic nanomagnets in the presence of thermal fluctuations

J. Appl. Phys. **112**, 023914 (2012)

Emergence of giant magnetic anisotropy in freestanding Au/Co nanowires

Appl. Phys. Lett. **101**, 043108 (2012)

Enhanced magnetic and dielectric properties of Eu and Co co-doped BiFeO₃ nanoparticles

Appl. Phys. Lett. **101**, 042401 (2012)

Demonstration of laser induced magnetization reversal in GdFeCo nanostructures

Appl. Phys. Lett. **101**, 022410 (2012)

Additional information on *Appl. Phys. Lett.*

Journal Homepage: <http://apl.aip.org/>

Journal Information: http://apl.aip.org/about/about_the_journal

Top downloads: http://apl.aip.org/features/most_downloaded

Information for Authors: <http://apl.aip.org/authors>

ADVERTISEMENT

AEROTECH
nano Motion Technology

Click here for the **FREE**
nano Motion Technology Catalog

Linear Single-Axis and Dual-Axis Stages

Rotary Stages

Goniometers

Vertical Lift and Z Stages

The advertisement features a blue background with a white wave-like pattern at the bottom. It displays four categories of motion technology products: Linear Single-Axis and Dual-Axis Stages, Rotary Stages, Goniometers, and Vertical Lift and Z Stages. Each category is accompanied by images of the respective hardware. On the right side, there is a vertical image of the 'nano Motion Technology' catalog, which lists key features: Long Travel, High Dynamic Performance, High Accuracy, High Resolution, and Easy-to-Use Software. The Aerotech logo is visible in the bottom right corner of the catalog image.

Room temperature magnetic stabilization of buried cobalt nanoclusters within a ferromagnetic matrix studied by soft x-ray magnetic circular dichroism

A. T. Hindmarch,^{1,a)} K. J. Dempsey,¹ J. P. Morgan,¹ B. J. Hickey,¹ D. A. Arena,² and C. H. Marrows¹

¹*School of Physics & Astronomy, E. C. Stoner Laboratory, University of Leeds, Leeds LS2 9JT, United Kingdom*

²*National Synchrotron Light Source, Brookhaven National Laboratory, Upton, New York 11973, USA*

(Received 8 August 2008; accepted 10 October 2008; published online 29 October 2008)

Single dusting layers of size-selected Co nanoclusters (NCs) of sizes ranging from 1.5–5.5 nm have been deposited by a gas-phase aggregation method in ultrahigh vacuum, and embedded within a NiFe matrix. Magnetic hysteresis loops have been obtained using soft x-ray magnetic circular dichroism, which shows that these Co NCs embedded in NiFe exhibit room temperature ferromagnetism with identical coercivity to the surrounding NiFe film. The strong local exchange field at the interface between NiFe and Co NCs, combined with the magnetic anisotropy of the NiFe film, allows stabilization of NC ferromagnetism which persists to room temperature. © 2008 American Institute of Physics. [DOI: 10.1063/1.3012368]

The study of magnetic nanoclusters (NCs) is gaining interdisciplinary popularity due to the potential of these systems for wide-ranging applications.¹ In ultrahigh density data storage, a fundamental limit on the areal data density arises. As the size of magnetic NC “bits” decreases the magnetocrystalline anisotropy energy, the product of magnetocrystalline anisotropy energy density K_V and volume V falls. The “blocking temperature” T_B is typically defined as $k_B T_B \sim n_\tau K_V V$, where n_τ relates to the timescale over which the reversal occurs. At temperatures above T_B , the orientation of the NC magnetic moment is unstable over a timescale τ as the anisotropy can no longer compete with thermal fluctuations; it can no longer be used to encode and store data.²

Exchange bias has previously been used to stabilize the ferromagnetic (FM) moment by embedding layers of Co NCs within a film of antiferromagnetic (AF) CoO in order to enhance T_B .³ NC ferromagnetism then persists up to the Néel temperature of the AF matrix, in that case ≈ 290 K, with enhanced coercivity. For multiple layers of NCs embedded within an AF matrix, it is relatively simple to study the magnetic behavior of the NC ensemble by traditional magnetometry methods as the AF itself has no net magnetic moment.

A more experimentally challenging problem is to unambiguously determine the behavior of a *single* dusting layer of NCs embedded within a FM matrix. In this case, difficulty arises due to the fact that the total magnetization due to the NC dusting layers is small in comparison to that of the surrounding matrix, making it practically impossible to resolve using traditional magnetometry techniques. From a technological standpoint, the study of single NC layers is of much greater relevance as they are candidates for, e.g., data storage media or processing elements. Coupling to a FM matrix should enhance T_B further over coupling to an AF as FMs typically have significantly higher critical temperatures than AFs: this should providing more stable—and manipulable—NC moments.

Here, we report a study using a single NC dusting layer embedded within a FM matrix, measured by soft x-ray magnetic circular dichroism (SXMCD),⁴ a technique which allows *element specific* study of the magnetic moments and anisotropies of magnetic nanostructures.⁵ Similar measurements have previously been performed on Fe NCs covered with a thin Co overlayer,⁶ where NC ferromagnetism was observed to temperatures of ~ 50 K but without a strong exchange interaction between NCs and FM overlayer. Here we demonstrate a strong interfacial exchange coupling between NiFe FM matrix and Co NCs, which allows the magnetocrystalline anisotropy of the FM film to stabilize the NC magnetic moment at least to room temperature.

Samples were deposited in a custom ultrahigh vacuum system equipped with a commercial size-selected NC deposition source.⁷ This produces NCs by gas-phase aggregation of sputtered material flux in a differentially pumped aggregation zone, similar to that described in Ref. 8. The NC size distribution is determined by parameters such as aggregation length, discharge power, Ar pressure, and He flow. After emerging from the aggregation zone, charged clusters, which constitute around 30%–50% of the NC flux, are size selected by passing through a quadrupole mass filter (QMF) and deflected by a transverse electric field toward an offset substrate. The QMF may be used either to measure the NC size distribution, as shown in the inset of Fig. 1, or to selectively pass only those clusters within a specified size window.⁸

All samples were deposited onto pieces cut from a Si(001) wafer, and contain single dusting layers of size-selected Co NCs of diameter (1.5 ± 0.1) nm (total of 128–195 atoms), (3.5 ± 0.1) nm (1902–2260 atoms), or (5.5 ± 0.1) nm (7719–8640 atoms); the NC coverage was intentionally low in order to avoid intercluster interactions.⁹ The structures used for our SXMCD investigations were Si/SiO/Co NC/Al[15 Å] (clean NC), Si/SiO/NiFe[200 Å]/Co NC/NiFe[30 Å]/Al[15 Å] (embedded NC), and Si/SiO/NiFe[200 Å]/Co NC/Al[15 Å] (surface NC). Al capping has been shown to have no influ-

^{a)}Electronic mail: a.t.hindmarch@leeds.ac.uk. Website: http://www.stoner.leeds.ac.uk.

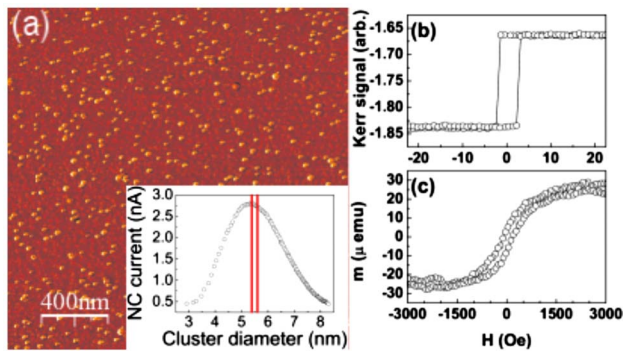


FIG. 1. (Color online) (a) $2 \times 2 \mu\text{m}^2$ AFM image of a dusting layer of 5.5 nm Co NCs. The inset shows a QMF size-distribution scan of the Co NC flux, with the mass filter bandpass window— $(5.5 \pm 0.1) \text{ nm}$ —indicated by vertical red lines. (b) Room temperature MOKE hysteresis loop of a NiFe film. (c) VSM hysteresis loops for a clean dusting layer of 5.5 nm Co NCs, showing FM behavior at 25 K (note the different field scales).

ence on the magnetic properties of Co NCs.¹⁰ Samples of Si/SiO/CoFeB[200 Å]/Co NC were deposited for atomic force microscope (AFM) imaging. All metallic thin-film layers were deposited by dc magnetron sputtering in a 2.7 mTorr Ar atmosphere and alloy sputtering targets of compositions Ni₈₀Fe₂₀ and Co₄₀Fe₄₀B₂₀ were used. A 150 Oe magnetic field was applied in the sample plane during deposition.

Conventional magnetic measurements were made at room temperature by longitudinal magneto-optical Kerr effect (MOKE) using a HeNe laser with spot diameter $\sim 0.5 \text{ mm}$ and at low temperatures using a variable temperature vibrating sample magnetometer (VSM). The quoted instrument sensitivity of the VSM is better than $6 \times 10^{-6} \text{ emu}$ at room temperature, and improves slightly with decreasing temperature. The field sweep rates during MOKE and VSM measurements were ~ 2 and $\sim 25 \text{ Oe/s}$.

SXMCD measurements were made at the U4B beamline at NSLS, Brookhaven. The beamline was operated with a circular polarization of 90% and an energy resolution of $\sim 1.5 \text{ eV}$ at the Co L_{III} edge. The data were collected by monitoring the sample drain current as a function of incident photon energy, normalized to the incident photon flux. The photon beam was incident at 45° to the sample normal and the applied magnetic field was in plane. All SXMCD measurements were made at room temperature.

Reversing the sample magnetization allows the photon to couple either to majority or minority spin. This produces parallel (μ^+) and antiparallel (μ^-) absorption spectra from which a SXMCD difference spectrum, $\mu^+ - \mu^-$, is derived.¹¹ The μ^\pm are measured in an applied hold field of $\pm 10 \text{ Oe}$ after applying a pulsed field of $\pm 2.5 \text{ kOe}$. Element specific SXMCD hysteresis loops are recorded by setting the incident beam energy close to maximum dichroic signal on the Co or Fe L_{III} edge, and then recording the electron yield while sweeping the magnetic field. In this geometry, the applied magnetic field is limited to $\sim 100 \text{ Oe}$ to avoid Lorentz deflection of the sample drain current. All SXMCD measurements were made in a single pass with 2 s integration time for measurements on embedded NC samples and 1 s integration for the matrix background, bulk reference, and surface NC samples.

Figure 1(a) shows a $2 \times 2 \mu\text{m}^2$ AFM image of a dusting layer of 5.5 nm Co NCs deposited on a CoFeB underlayer—this provides a smooth, essentially featureless, background to

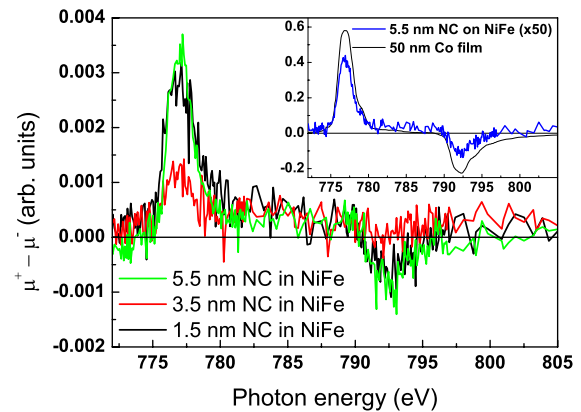


FIG. 2. (Color online) Room temperature SXMCD spectra for dusting layers of Co NCs embedded in NiFe. Differences in SXMCD signal strength primarily reflect variation in Co NC dusting coverage. Inset are the spectra for a Co film and a dusting of Co NCs on NiFe.

the image and prevents NCs readily adhering to the tip. While tip convolution makes it impossible to determine the NC size, we see that the NC coverage is around $150 \text{ clusters}/\mu\text{m}^2$, significantly lower than the $\sim 10^4 - 10^5 \text{ clusters}/\mu\text{m}^2$ typically observed for NC ensembles self-assembled on a surface during submonolayer deposition.^{9,12,13}

Initial magnetic characterization of the NiFe matrix film and clean NC dusting layers was performed by MOKE magnetometry and variable temperature VSM. Figure 1(b) shows a MOKE hysteresis loop of a NiFe [200 Å] reference film without NC dusting. The film shows 100% remanence with a coercive field $H_C \approx 2.5 \text{ Oe}$, typical of sputtered NiFe. The Co NCs studied here are all below the 7 nm limit for single-domain behavior,¹⁴ and 5.5 nm Co NCs typically have $T_B < 100 \text{ K}$.¹⁵ Measuring T_B of single Co NC dusting layers by VSM is nontrivial as the magnetic moment of the NC dusting is close to the instrument sensitivity. A VSM hysteresis loop at 25 K is shown in Fig. 1(c), showing that clean 5.5 nm Co NCs are FM with $H_C \approx 130 \text{ Oe}$ and remanence $\sim 25\%$. All clean Co NC samples are superparamagnetic at room temperature (not shown). We point out that temperature dependent changes in both NC anisotropy and magnetic moment must be considered when comparing thermal activated behavior at different temperatures.

The SXMCD spectra for single dusting layers of Co NCs embedded in NiFe are shown in Fig. 2. The signals are orders of magnitude weaker than that from a 500 Å Co reference film (inset) due to the small volume of Co present in the samples; they are also roughly a factor of 4 smaller than measured for NiFe/surface NC (also shown in the inset, magnified) due to the photoelectron escape depth attenuating the electron yield from embedded NCs. The bulk Co reference spectrum compares well with the literature, e.g., Ref. 11. No background subtractions have been made to any of the μ^\pm absorption spectra prior to deriving the SXMCD difference spectra. No dichroism signal is observed between the μ^\pm for clean NC samples at room temperature; as the $\pm 10 \text{ Oe}$ hold field causes no net rearrangement of the randomly oriented superparamagnetic NC magnetic moments, the μ^\pm are equivalent: this is confirmed by VSM measurements (not shown).

Although the μ^\pm and SXMCD signals from the embedded Co NC dusting layers are small, making reliable appli-

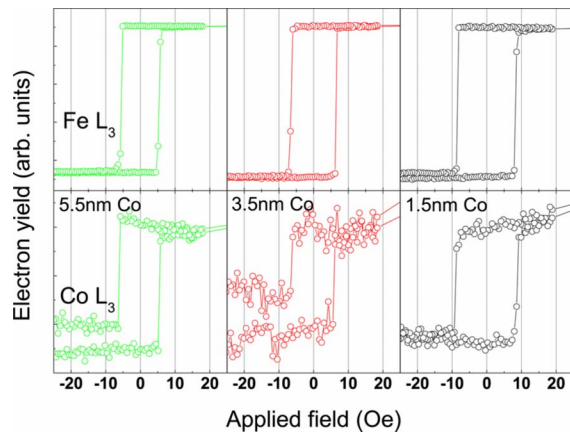


FIG. 3. (Color online) Room temperature SXMCD hysteresis loops for single Co NC dusting layers embedded in NiFe, measured at the Fe (NiFe matrix, upper frames) and Co (NC dusting layer, lower frames) L_{III} absorption edges.

cation of the XMCD sum rules¹¹ difficult, there is a clear dichroism at both the L_{II} and L_{III} absorption edges which appear at photon energies close to 792.5 and 777 eV, respectively. This indicates not only that we are able to probe magnetism in a single dusting layer of NCs buried below 30 Å of NiFe (in addition to 10 Å of Al) using electron yield SXMCD but also that there is a net magnetization of the embedded Co NC dusting layer in a ± 10 Oe applied field, i.e., the embedded Co NCs are *no longer* superparamagnetic at room temperature in the presence of a 10 Oe applied magnetic field.

Unambiguous demonstration that embedded Co NCs are indeed FM at room temperature is provided by the SXMCD hysteresis loops at the Co L_{III} edge, shown in the lower frames of Fig. 3. No background subtractions or drift correction has been applied to the hysteresis loops. In each case, a clearly FM hysteresis loop is observed for the Co NC dusting layer, with around 100% remanence and $H_C < 10$ Oe; entirely dissimilar to hysteresis loops for clean Co NCs in either the superparamagnetic or FM phases, but reminiscent of the hysteresis loop for a clean NiFe film, are shown in Fig. 1. For each sample, a SXMCD hysteresis loop of the NiFe matrix was also measured at the Fe L_{III} edge, shown in the upper frames of Fig. 3. These do not differ significantly from the hysteresis loop of a clean NiFe film shown in Fig. 1. The correspondence between the coercive fields measured at Co and Fe absorption edges in Fig. 3 is immediately apparent. For samples with 1.5, 3.5, and 5.5 nm NCs, the coercive field measured at the Co (Fe) absorption edge is 8.5 (8.0) Oe, 6.2 (6.5) Oe, and 5.6 (5.4) Oe, respectively: in each case identical within the ~ 0.5 Oe experimental resolution.

The obvious explanation for this correspondence in coercivity between Co NCs and the surrounding NiFe matrix is, of course, that there is strong interfacial magnetic coupling: the interface coupling interaction is FM as the dichroism has the same sign at the Co and Fe absorption edges. Such coupling has, for example, been observed previously in thin NiFe/Co films.¹⁶ Noncollinear interfacial moments have also previously been observed in FM films;¹⁷ this may introduce a small, e.g., biquadratic interfacial coupling term, resulting in canting of the net cluster moment from that of the NiFe film. However, we see no evidence of this from any of our measurements on these films.

In summary, we have demonstrated, using SXMCD spectroscopy and hysteresis measurements, a strong interfacial exchange coupling between Co NCs and a surrounding NiFe matrix. This exchange coupling allows the magnetocrystalline anisotropy of the NiFe matrix to enhance the effective anisotropy of the Co NCs, allowing stabilization of NC ferromagnetism, with identical coercivity to the NiFe matrix, which persists *at least* to room temperature.

The authors acknowledge financial support from EPSRC and are grateful to Brookhaven National Laboratory for the provision of NSLS beamtime.

¹S. D. Bader, *Rev. Mod. Phys.* **78**, 1 (2006).

²D. A. Thompson and J. S. Best, *IBM J. Res. Dev.* **44**, 311 (2000).

³V. Skumryev, S. Stoyanov, Y. Zhang, G. Hadjipanayis, D. Givord, and J. Nogues, *Nature (London)* **423**, 850 (2003).

⁴J. Stöhr, *J. Magn. Magn. Mater.* **200**, 470 (1999).

⁵A. T. Hindmarch, C. J. Kinane, M. MacKenzie, J. N. Chapman, M. Henini, D. Taylor, D. A. Arena, J. Dvorak, B. J. Hickey, and C. H. Marrows, *Phys. Rev. Lett.* **100**, 117201 (2008).

⁶K. W. Edmonds, C. Binns, S. H. Baker, M. J. Maher, S. C. Thornton, O. Tjernberg, and N. B. Brookes, *J. Magn. Magn. Mater.* **220**, 25 (2000).

⁷See <http://www.oaresearch.co.uk/oaresearch>.

⁸S. H. Baker, S. C. Thornton, A. M. Keen, T. I. Preston, C. Norris, K. W. Edmonds, and C. Binns, *Rev. Sci. Instrum.* **68**, 1853 (1997).

⁹E. Gu, S. Hope, M. Tselepi, and J. A. C. Bland, *Phys. Rev. B* **60**, 4092 (1999).

¹⁰C. Clavero, L. Martinez, A. Garcia-Martin, J. M. Garcia-Martin, Y. Huttel, N. D. Telling, G. van der Laan, A. Cebollada, and G. Armelles, *Phys. Rev. B* **77**, 094417 (2008).

¹¹C. T. Chen, Y. U. Idzerda, H. J. Lin, N. V. Smith, G. Meigs, E. Chaban, G. H. Ho, E. Pellegrin, and F. Sette, *Phys. Rev. Lett.* **75**, 152 (1995).

¹²J. T. Lau, A. Fohlisch, R. Nietubyc, M. Reif, and W. Wurth, *Phys. Rev. Lett.* **89**, 057201 (2002).

¹³Y. Nogi, H. Wang, F. Ernult, K. Yakushiji, S. Mitani, and K. Takahashi, *J. Phys. D* **40**, 1242 (2007).

¹⁴M. E. Schabes, *J. Magn. Magn. Mater.* **95**, 249 (1991).

¹⁵S. P. Gubin and Y. A. Koksharov, *Inorg. Mater.* **38**, 1085 (2002).

¹⁶A. K. Suszka, C. J. Kinane, C. H. Marrows, B. J. Hickey, D. A. Arena, J. Dvorak, A. Lamperti, B. K. Tanner, and S. Langridge, *Appl. Phys. Lett.* **91**, 132510 (2007).

¹⁷A. T. Hindmarch, C. J. Kinane, C. H. Marrows, B. J. Hickey, M. Henini, D. Taylor, D. A. Arena, and J. Dvorak, *J. Appl. Phys.* **101**, 09D106 (2007).